Korean J. Chem. Eng., **30**(2), 440-447 (2013)
DOI: 10.1007/s11814-012-0130-0

Kinetic and thermodynamic study of Eu(III) sorption on natural red earth in South China

Tao Yu*,†, Wang-Suo Wu, Zhi-Rong Liu*, Si-Wei Zhang*, and Zheng-Wei Nie***

*College of Chemistry, Biology and Materials Science, East China Institute of Technology, Fuzhou 344000, Jiangxi, P. R. China
**Radiochemistry Laboratory, School of Nuclear Science and Technology, Lanzhou University, Lanzhou 730000, Gansu, P. R. China
(*Received 21 April 2012 • accepted 12 August 2012*)

Abstract−We did a kinetic and thermodynamic study of Eu(III) sorption on natural red earth (NRE) in South China as a function of contact time, pH values, ionic strength, humic acid (HA) and temperature under ambient conditions. Linear and nonlinear regression methods in selecting the optimum sorption isotherm were applied on the experimental data. The results suggest that sorption of Eu(III) on NRE can be described by a pseudo-second-order rate equation and strongly dependent on ionic strength at pH<7. Sorption of Eu(III) on NRE increased with increasing temperature, two-parameter and three-parameter isotherms were applied to analysis the equilibrium adsorption data, and a comparison of linear and nonlinear regression methods was done. The thermodynamic parameters (ΔH^0, ΔS^0 and ΔG^0) of Eu(III) sorption on NRE at different temperatures were calculated from the temperature-dependent sorption isotherms, indicating that the sorption process of Eu(III) was spontaneous. The results showed that the nonlinear method is a better way to obtain the isotherm parameters and the data were in good agreement with the Freundlich isotherm model.

Key words: Kinetic, Thermodynamic, Sorption, Eu(III), NRE

INTRODUCTION

The sorption and migration of radionuclides in soils and clay minerals have received more and more attention because the removal of radioactive waste has a huge effect on the environment [1]. Europium (Eu(III)) is one of the lanthanides and its ion is used to be treated as a trivalent actinide analogue, and the sorption characteristics of Eu(III) on soils, clay minerals and oxides have been studied in worldwide [2]. Many factors influence the sorption such as pH, ionic strength, humic substances, temperature, chemical and mineralogical nature of adsorbents and chemical species of cations, etc. Beneš et al. [3] studied the kinetics of sorption of Eu(III) on sandy sediment through a radiotracer method in batch experiments, and the results showed that the kinetics and mechanism of the sorption strongly depend on pH; Eu(III) was sorbed mainly as humate complex from the solution of humic acid at pH 4.8 and carbonate complexes were the probable forms sorbed at pH 8.8. Štamberg et al. [4] used a verified model to describe the sorption of Eu(III)-Aldrich humic acid system at pH 4 and 7, and indicated that the complexation proceeds by consecutive bonding of cationic forms on the macromolecule (HA), until its negative charge formed due to dissociation of its carboxyl groups is fully neutralized. Hu et al. [5] studied sorption of Eu(III) on Na-bentonite in the absence/presence of humic acid (HA). The results showed that the sorption of Eu(III) on Na-bentonite was dependent on pH values; the presence of HA had little effect on Eu(III) sorption at low pH values, but decreased Eu(III) sorption at high pH values.

†To whom correspondence should be addressed.
E-mail: xiaoshan770@163.com

Clay minerals have many sorption characteristics such as ion exchange capability, expanding capacity, high capability of adsorbing pollutants and self-purification functions; therefore, clay minerals have the capacity for controlling environmental pollution [6]. Red earth has two important compositions influencing the sorption: iron oxides and organic matter (OM). Dong et al. [7] investigated characteristics of sorption and desorption of Eu(III) on red earth by batch method and the column method, and found the sorption significantly depends on pH and fulvic acid (FA). The iron oxides content of the red earth had a negative contribution to the sorption, and the humic substance and high pH have a great tendency to immobilize Eu(III) on red earth. Tao et al. [8] researched the sorption of Am(III) on a red earth and three kinds of treated red earth samples. The results showed pH, ionic strength and fulvic acid (FA) have strong effects on the Am(III) sorption; OM has a positive contribution and iron oxides have a high negative influence on the Am(III) sorption by the untreated red earth. The sorption-desorption of copper at contaminated levels in two red earths was investigated. The results suggest that the red earth derived from the quaternary red earths (REQ) adsorbed more Cu^{2+} than the sample developed on the arenaceous rock (RAR), and the sorption of Cu^{2+} decreased soil pH, the distribution coefficient (K_d) decreased with the addition of Cu^{2+}; in addition, most of the adsorbed Cu^{2+} in the earths was desorbed in the NH_4Ac [9]. Mahatantila et al. [10] studied the sorption of lead(II) on natural red earth (NRE) from its iron and aluminum oxide forms as a function of pH, ionic strength, initial sorbent and sorbate concentrations and time, and found that the rate of sorption of lead(II) is very fast and follows the pseudo-second-order model. Lead(II) sorption on NRE is better explained by Langmuir-Freundlich isotherm and a mixture of monodentate and bidentate surface com-

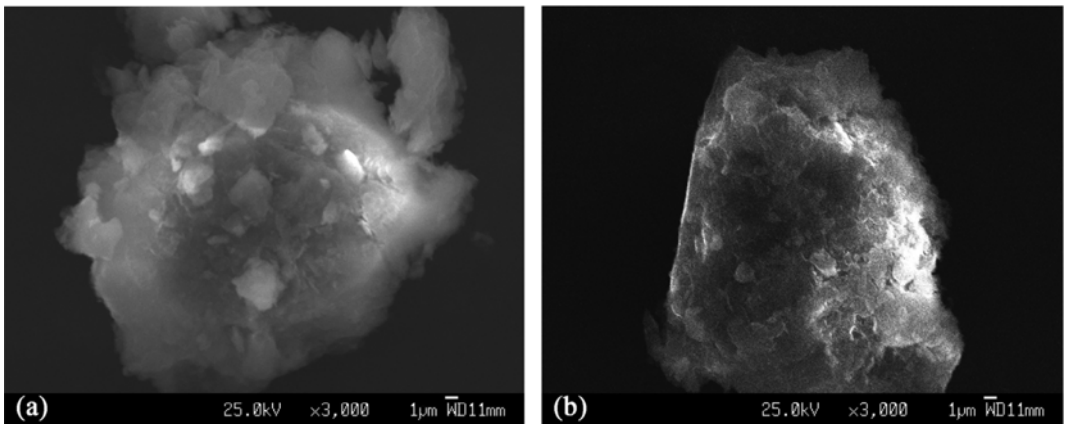

Fig. 1. SEM micrographs of NRE (a) and Eu(III)-NRE (b).

plexes forms within Pb(II) and surface sites of NRE.

The main objectives of this paper are: (1) to collect and prepare natural red earth (NRE) sample; (2) to characterize NRE using XRD and SEM; (3) to study the sorption kinetics and thermodynamics of Eu(III) sorption on NRE by linear and nonlinear methods; (4) to study the sorption of Eu(III) on NRE as a function of contact time, pH, ionic strength, foreign ions and humic acid (HA); and (5) to discuss the sorption mechanism of Eu(III) on NRE.

EXPERIMENTAL

1. Materials

Materials and reagents used in the experiments are analytical grade. The sample of natural red earth was derived from the surface horizon (0-10 cm) at Linchuan county, Fuzhou city, Jiangxi province (China) and was ground to grain size of <0.01 mm.

Chemical components of the natural red earth analyzed by X-ray diffraction (XRD) were: SiO_2 68.82%, Al_2O_3 14.47%, Fe_2O_3 5.16%, TiO_2 0.903%, K_2O 1.36%, Na_2O 0.58%, CaO 0.156%, MgO 0.29%, MnO 0.015%, loss on ignition 8.15%.

Eu(III) was purchased from Ganzhou Deshipu Advanced Material Resource Co., LTD. (Jiangxi province, China), and humic acid and arsenazo III purchased from Chengdu Xiya Chemical Technology Co., LTD. (Sichuan province, China).

2. Characterization

The surface properties of NRE were characterized by X-ray diffraction and scanning electron microscope (SEM). XRD analysis was performed with Cu K_α radiation (λ=0.15406 nm) with a Rigaku diffractometer. The operation conditions of XRD were 36 kV and 20 mA.The 2θ rate was 10°-90°. Patterns were identified by comparison to the JCPD standards. The morphology of NRE samples was studied by scanning electron microscopy at 25 kV.

3. Sorption Procedures

The experiments were all under the normal conditions. The sorption experiments of Eu(III) on NRE were carried out at three temperatures: 30 °C, 45 °C, 60 °C, respectively. The stock solutions of NRE, NaCl, HA, Eu(III) solution were added in the polyethylene tubes to achieve the desired concentrations. The solid and liquid phases were separated by centrifugation at 6,000 rpm for 30 min after the suspensions are shaken for 12 h. The counts of Eu(III) with arsenazo III were analyzed by a spectrophotometer, and the sorption percentage (S) was calculated according to Eq. (1).

The sorption percentage and the distribution coefficient (K_d) are calculated from the following equations [5]:

$$S\% = \left(1 - \frac{A_{eq}}{A_s}\right) \times 100\% \quad (1)$$

$$K_d = \frac{C_s}{C_{eq}} \times \frac{V}{m} \quad (2)$$

where A_{eq} is the activity of Eu(III) in liquid phase and A_s is that of Eu(III) in solid phase, C_s is the concentration of Eu(III) on solid phase (mol/g), C_{eq} is the concentration of Eu(III) in liquid phase (mol/L), V is the volume of the suspension and m is the mass of NRE. The values of C_s and C_{eq} were calculated by a standard curve of absorbance.

RESULTS AND DISCUSSION

1. SEM Characterization

SEM micrographs of NRE and Eu(III)-NRE (after sorption reaction) are shown in Fig. 1. From Fig. 1, before the sorption reaction, NRE (Fig. 1(a)) shows a layer structure and some pieces pile up, and the size of a certain single piece is about 1.0-5.0 μm in width.

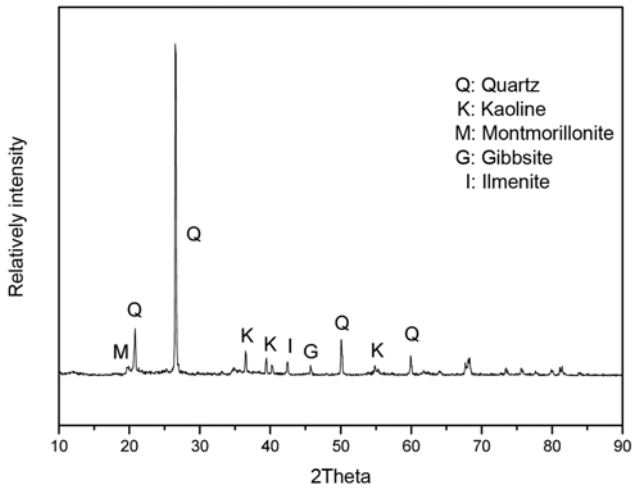

Fig. 2. XRD pattern of NRE.

Compared with NRE, the structure of Eu(III)-NRE is not changed obviously (Fig. 1(b)), while the sorption sites reduce and the sorption reaction made the shape of NRE regular and orderly.

2. XRD Analysis

Fig. 2 shows the XRD pattern of NRE. The main peaks correspond to the crystal structure of kaoline and quartz; the other peaks correspond also including gibbsite, montmorillonite and ilmenite, *etc*. This suggests that the composition of NRE is very complex, and the sorption influence factors will be as much as expected.

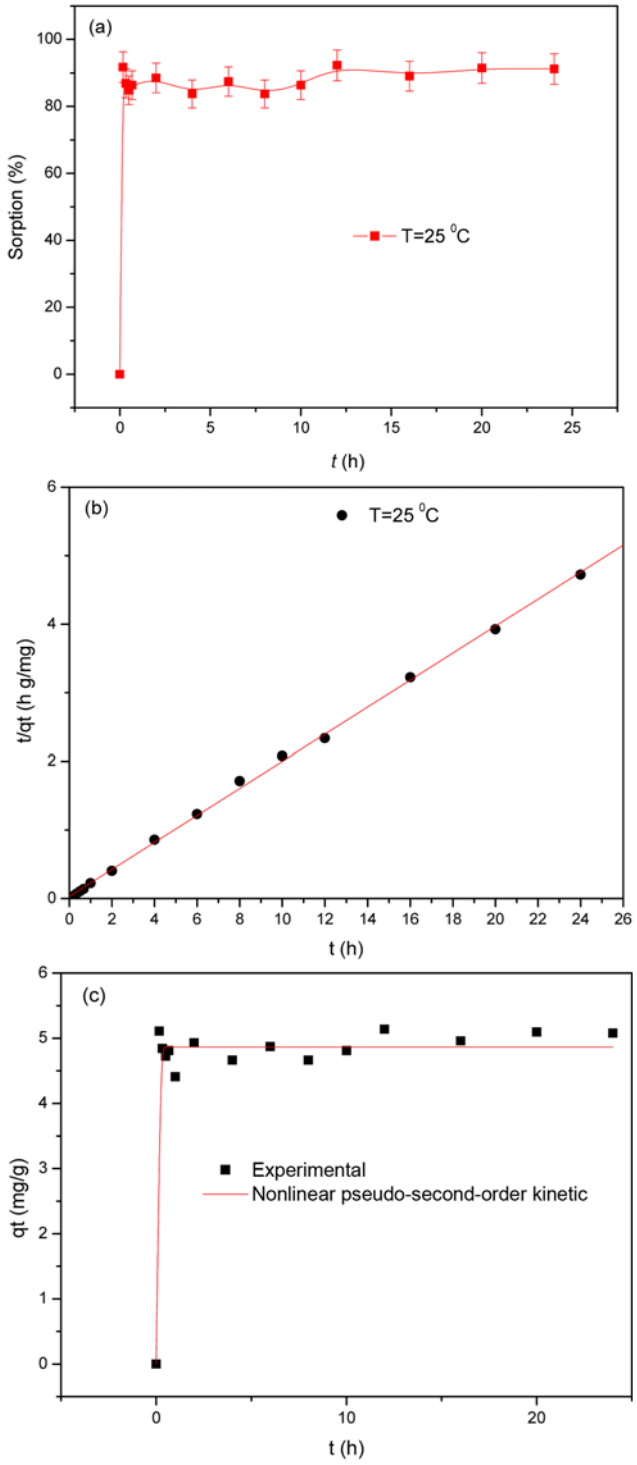

Fig. 3. Sorption of Eu(III) as a function of contact time (a) and the linear(b) and nonlinear (c) pseudo-second-order kinetic of Eu(III) sorption on NRE. pH=6.50±0.05, m/V=1.0 g/L.

3. Effect of Contact Time

Fig. 3(a) shows the removal of Eu(III) from solution to NRE as a function of contact time. The sorption of Eu(III) achieves the sorption equilibrium for about 12 hours; after 12 hours, the removal percent of Eu(III) maintains a constant level with increasing contact time. Twelve hours was selected as equilibrium time in the following experiments. There is an increase-decrease progress before the sorption achieved equilibrium (t<2 h), which indicates that sorption of Eu(III) on NRE is mainly attributed to physical sorption rather than chemical sorption in initial 1 h; however, the chemical sorption dominates in the following time. Here, a pseudo-second-order rate equation is used to simulate the kinetic sorption to analyze the sorption percentage of Eu(III) on NRE [11,12]:

$$\frac{t}{q_t} = \frac{1}{K' q_e^2} + \frac{1}{q_e} t \quad (3)$$

where K' (g/mg/h) is the pseudo-second-order rate constant of sorption, q_t (mg/g of dry weight) is the amount of Eu(III) adsorbed on the surface of NRE at time t (h), and q_e (mg/g) is the equilibrium sorption capacity.

While, there are four linear forms and a nonlinear form of pseudo-second-order kinetics, and the different linearized forms of the pseudo-second-order equation are given in Table 1 [13,14].

Chi-square (x^2) tests were used as an error function assessment to evaluate the fit of the equations to the experimental results [13]:

$$x^2 = \sum \frac{(q_e' - q_e)^2}{q_e} \quad (4)$$

where q_e' (mg/g) and q_e (mg/g) are the measured and calculated sorption capacity at equilibrium. Fig. 3(b) shows that linear plot feature of t/q_t vs. t is achieved. In addition, the correlation coefficient (R) is very close to 1, which suggests that the pseudo-second-order rate equation could describe the kinetic sorption well. Through duplicate experiments of every site in Fig. 3, the overall experimental error is less than 5%.

The linear forms of type 2-4 were drawn and the results indicated that the linear of the three types to the experimental data are very weak. While, nonlinear analysis is adopted for analyzing the experimental data to avoid the drawbacks of linear method. The nonlinear method for the sorption of Eu(III) on NRE is shown in Fig. 3(c). The pseudo-second-order kinetic parameters of linear form (type 1) and nonlinear form, K', q_e and x^2 are listed in Table 2.

From Table 2, the relatively low x^2 values of the nonlinear pseudo-second-order expression show that compared to the linear forms, the nonlinear pseudo-second-order kinetic expression could fit the kinetics of Eu(III) on NRE better.

4. Effect of Solid-to-liquid Ratio (m/V)

Fig. 4 shows the sorption of Eu(III) on NRE as a function of solid-to-liquid ratios (m/V), and K_d is shown in the same figure. The sorption percentage of Eu(III) is increasing with the increasing of m/V. With the increasing of NRE content, more sorption sites are applied to participate in the sorption process of Eu(III), and the removal percent of Eu(III) increases, too [15,16]. On the contrary, values of K_d show the opposite tendency; in the range of m/V<0.5 g/L, K_d

Table 1. Linear forms of pseudo-second-order kinetics

Type	Nonlinear form	Linear form	Plot	Parameters
1	$q_t=\frac{K'q_e^2t}{1+K'q_et}$	$\frac{t}{q_t}=\frac{1}{K'q_e^2}+\frac{1}{q_e}t$	t/q_t vs. t	q_e=1/slope K'=slope^2/intercept
2		$\frac{1}{q_t}=\frac{1}{q_e}+\frac{1}{K'q_e^2}\frac{1}{t}$	$1/q_t$ vs. $1/t$	q_e=1/intercept K'=intercept^2/slope
3		$q_t=q_e-\frac{1}{K'q_e}\frac{q_t}{t}$	q_t vs. q_t/t	q_e=intercept K'=1/(intercept×slope)
4		$\frac{q_t}{t}=K'q_e^2-K'q_eq_t$	q_t/t vs. q_t	q_e=intercept/slope K'=slope^2/intercept

Table 2. Linear and nonlinear methods' pseudo-second-order kinetic parameters for sorption of Eu(III) on NRE

Kinetic method	q_e (mg/g)	K' (g/mg/h)	x^2
Linear method (type1)	5.079	1.169	0.1156
Nonlinear method	4.865	1.563	0.0433

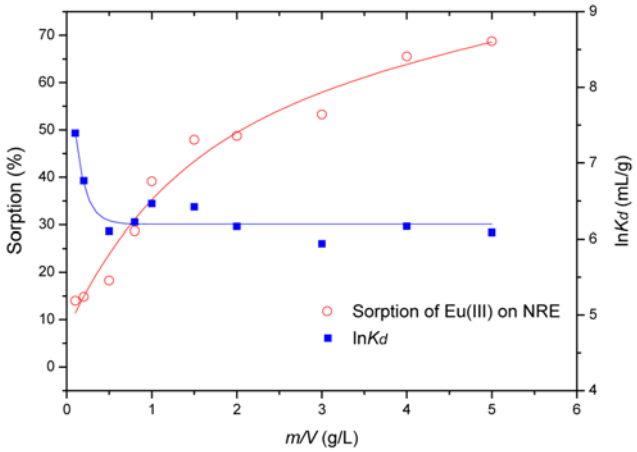

Fig. 4. Sorption of Eu(III) on NRE as a function of solid-to-liquid ratio: T=25±1 °C, pH=5.50±0.05, $C_{Eu(III)initial}$=4.40×10^{-4} mol/L.

decrease with the the increasing of m/V and maintain a constant level at m/V>0.5 g/L. The removal percent of Eu(III) achieves approximately 70% at m/V=5.0 g/L and approximately 14% at m/V=0.1 g/L. To avoid experimental error, the digital of m/V and sorption percentage could not be too big, neither too small; therefore, the solid-to-liquid ratio (m/V) is selected at m/V=1.0 g/L in the next sorption experiment.

5. Effect of pH and Ionic Strength

The pH values and ionic strength of the sorption system are very important influence factors for Eu(III) sorption. The removal percent of Eu(III) on NRE as a function of pH values in I=0, 0.01 M and 0.05 M NaCl, respectively, is shown in Fig. 5. Sorption of Eu (III) occurs at low pH values, and increases rapidly from ~10% to ~90% in the of range pH 3.0-7.0. At pH>7.0, the sorption of Eu(III) maintains a constant level with increasing pH. It indicates that the sorption of Eu(III) on NRE strongly depends on pH, and the surface complexation contributes to the sorption of Eu(III) on NRE. Sorption of I=0.01 M and 0.05 M NaCl is close and lower than I=0, which showed that ionic strength has a negative impact on sorption.

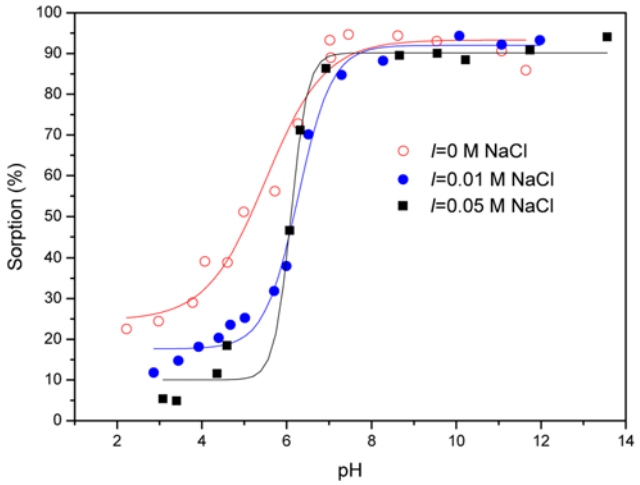

Fig. 5. Sorption of Eu(III) on NRE as a function of pH and ionic strength. T=25±1 °C, m/V=1.0 g/L. $C_{Eu(III)initial}$=4.40×10^{-4} mol/L.

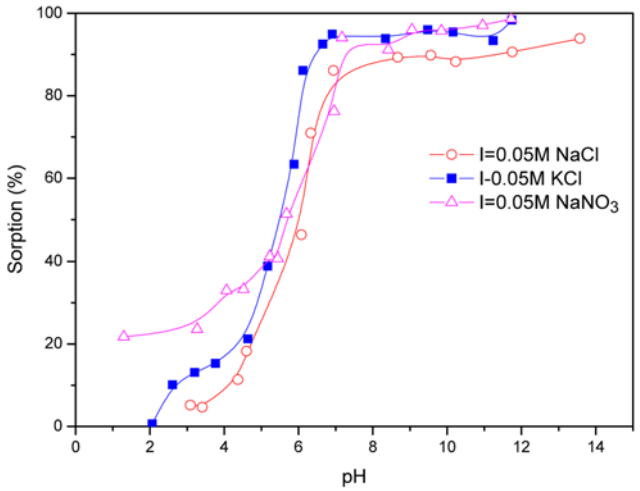

Fig. 6. Effect of different ions on the sorption of Eu(III) on NRE. $C_{Eu(III)initial}$=4.40×10^{-4} mol/L, T=25±1 °C, m/V=1.0 g/L.

The removal percent of Eu(III) from solution to NRE as a function of pH in different ions background electrolyte solutions is shown in Fig. 6. KCl and $NaNO_3$ have a little influence on the sorption of the system, compared to NaCl at the same concentration. The influence of anions shows the same characteristic that monoacidic ions have little influence on sorption, such as Cl^{-1} and NO_3^{-1}. These re-

sults indicate that surface complexation is obviously influenced by pH, and ion exchange reaction is influenced by ionic strength. At low pH, sorption of Eu(III) on NRE is dominated by ion exchange or outer-sphere complexation; while, at high pH, it is dominated by inner-sphere surface complexation [17,18].

According to the experiments, the mechanism of Eu(III) sorption on NRE is assumed [18-20]: The solid surface is assumed to be a number of variable charge sites (=S-OH), which could be either protonated and deprotonated. The sorption mechanism of Eu(III) on NRE can be presumed by the following reactions:

1) Ion exchange:

$$(=S\text{-}OH)+Eu^{3+} \Leftrightarrow (=S\text{-}O)Eu^{2+}+H^{+} \quad (5)$$

$$2(=S\text{-}OH)+Eu^{3+} \Leftrightarrow (=S\text{-}O)_2Eu^{+}+2H^{+} \quad (6)$$

$$3(=S\text{-}OH)+Eu^{3+} \Leftrightarrow (=S\text{-}O)_3Eu+3H^{+} \quad (7)$$

2) Sorption and hydrolysis at the surface of the NRE:

$$(=S\text{-}OH)+H_2O+Eu^{3+} \Leftrightarrow (S\text{-})Eu(OH)_2^{2+}+H^{+} \quad (8)$$

$$(=S\text{-}OH)+2H_2O+Eu^{3+} \Leftrightarrow (S\text{-})Eu(OH)_3^{+}+2H^{+} \quad (9)$$

$$(=S\text{-}OH)+3H_2O+Eu^{3+} \Leftrightarrow (S\text{-})Eu(OH)_4+3H^{+} \quad (10)$$

3) Hydrolysis of Eu^{3+} in solution:

$$Eu^{3+}+nH_2O \Leftrightarrow [Eu(OH)_m(H_2O)_{n-m}]^{3-m}+mH^{+} \quad (11)$$

being n>m, and exchange with hydrolyzed species:

$$(=S\text{-}OH)+[Eu(OH)_m(H_2O)_{n-m}]^{3-m} \Leftrightarrow (=S\text{-}O)-Eu(OH)_m^{2-m}+H^{+}+(n-m)H_2O \quad (12)$$

6. Effect of Humic Acid

Fig. 7 shows the effect of HA on the sorption of Eu(III) to NRE as a function of pH. The surface properties of NRE such as porous texture and charge are affected in the presence of humic acid [21]. The result shows that in the presence of HA at different concentrations, the sorption is enhanced at pH<7, and maintains a constant level at pH>7. The increase of Eu(III) sorption on HA-NRE hybrids in low pH region may be explained by a reduction in positive surface charge caused by the sorption of negatively charged HA at NRE surfaces, which results in a more favorable electrostatic environment for Eu(III) sorption and enhances the formation of ternary Eu-HA-NRE surface complexes [22].

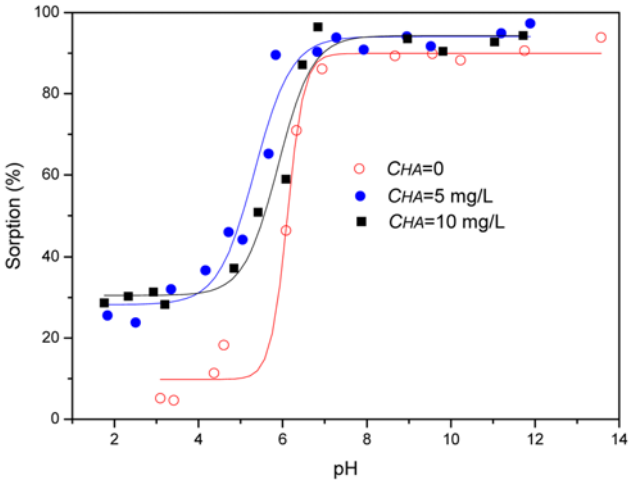

Fig. 7. Effect of HA on the sorption of Eu(III) to NRE as a function of pH values. T=25±1 °C, m/V=1.0 g/L, I=0.05 mol/L NaCl.

7. Sorption Isotherms

7-1. Linear Method

Several models could fit the sorption isotherm of Eu(III) on NRE by linear or nonlinear method. Two-parameter models, Freundlich and Langmuir models, and three-parameter models, Sips and Toth models were adopted to describe isotherms of the sorption as a function of temperature in order to understand the sorption mechanism. In addition, the Langmuir isotherm can be transformed to at least four linear forms. Models mentioned above are described in Table 1 [23-25].

where c_s (mol/g) is the equilibrium sorption capacity, c_{eq} is the concentration of Eu(III) in liquid phase (mol/L), c_{max} is the maximum sorption capacity (mol/g), b is a constant that relates to the heat of sorption, a and n are Freundlich constants.

Sorption isotherms of Eu(III) sorption at pH 6.5 are shown in

Table 3. Sorption isotherms in linear or nonlinear forms

Isotherms	Nonlinear	Linear	Plot	Parameters
Langmuir1	$c_s=\frac{bc_{max}c_{eq}}{1+bc_{eq}}$	$\frac{c_{eq}}{c_s}=\frac{1}{bc_{max}}+\frac{c_{eq}}{c_{max}}$	$\frac{c_{eq}}{c_s}$ vs. c_{eq}	b=slope/intercept c_{max}=1/slope
Langmuir2		$\frac{1}{c_s}=\left(\frac{1}{bc_{max}}\right)\frac{1}{c_{eq}}+\frac{1}{c_{max}}$	$\frac{1}{c_s}$ vs. $\frac{1}{c_{eq}}$	b=intercept/slope c_{max}=1/intercept
Langmuir3		$c_s=c_{max}-\left(\frac{1}{b}\right)\frac{c_s}{c_{eq}}$	c_s vs. $\frac{c_s}{c_{eq}}$	b=−1/slope c_{max}=intercept
Langmuir4		$\frac{c_s}{c_{eq}}=bc_{max}-bc_s$	$\frac{c_s}{c_{eq}}$ vs. c_s	b=−slope c_{max}=−intercept/slope
Freundlich	$c_s=ac_{eq}^{n}$	$\lg c_s=\lg a+n\lg c_{eq}$	$\lg c_s$ vs. $\lg c_{eq}$	a=exp(intercept) n=slope
Sips	$c_s=\frac{c_{max}(bc_{eq})^n}{1+bc_{eq}}$			
Toth	$q_e=\frac{c_{max}bc_{eq}}{(1+(bc_{eq})^n)^{1/n}}$			

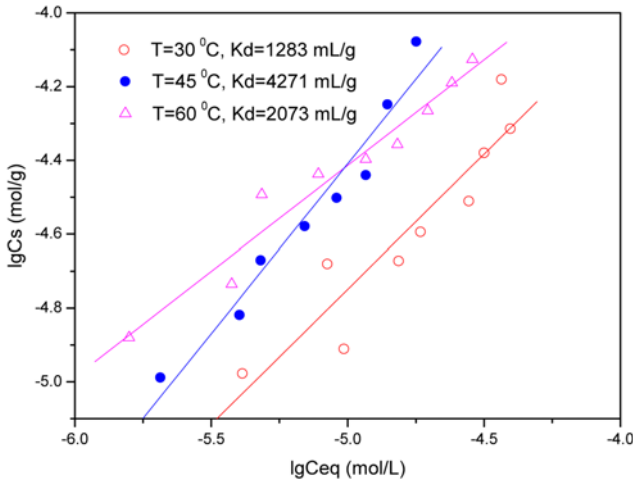

Fig. 8. Freundlich isotherms for Eu(III) sorption on NRE at three different temperatures: pH=6.50±0.05, m/V=1.0 g/L, I= 0.05 mol/L NaCl.

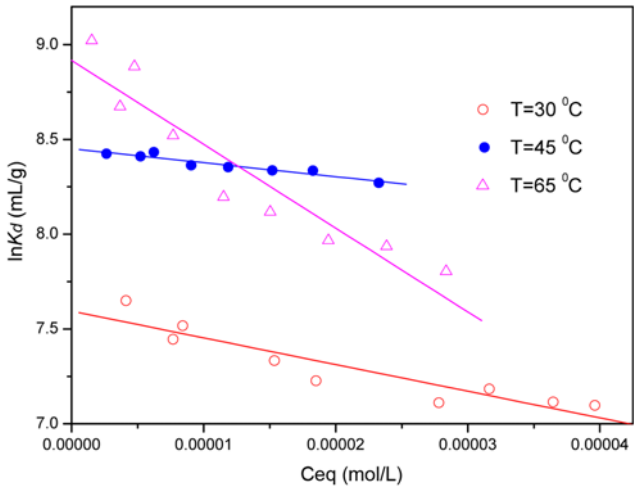

Fig. 9. Linear plots of $\ln K_d$ versus c_{eq}. pH=6.50±0.05, m/V=1.0 g/L, I=0.05 mol/L NaCl.

Table 4. Parameters of Langmuir, Freundlich isotherms by linear method

t/°C	Langmuir 1			Freundlich		
	c_{max}	b	R^2	a	n	R^2
30	1.3969×10^{-4}	1.3748×10^{4}	0.1559	0.0851	0.7321	0.8402
45	3.1125×10^{-4}	1.6153×10^{4}	0.0549	0.6378	0.8357	0.9444
60	9.9546×10^{-5}	7.0993×10^{4}	0.8592	0.0281	0.5729	0.9491

Fig. 8, and the values of K_d are in Fig. 8, too. The result shows that the sorption isotherm of Eu(III) on NRE at 60 °C is highest, and lowest at 30 °C, which indicates that Eu(III) sorption increases as the increasing temperature in the range of 30-45 °C, and decreases with increasing temperature in the range of 45-60 °C.

The related parameters have been listed in Table 4; Langmuir 2-4 models are not listed because of their weak linearity. The results indicate that the Freundlich model fitted to describe the sorption process better than the Langmuir model.

From Fig. 8, the linear correlations of Eu(III) sorption isotherms also confirm that Eu(III) sorption is a Freundlich model in observed conditions. With the increasing of temperature, the values of K_d are increasing obviously from 1,283 mL/g to 4,271 mL/g with temperature increasing from 30 °C to 45 °C, and decreasing from 4,271 mL/g to 2,073 mL/g with temperature increasing from 45 °C to 60 °C, which indicates that the temperature could enhance Eu(III) sorption in lower temperature range and weaken the sorption in higher temperature range.

The thermodynamic parameters (ΔG^0, ΔS^0, and ΔH^0) for Eu(III) sorption on NRE are calculated from the equations [26,27]:

$$\Delta G^0 = -RT\ln K \quad (16)$$

$$\left(\frac{\partial G^0}{\partial T}\right)_p = -\Delta S^0 \quad (17)$$

$$\Delta H^0 = \Delta G^0 + T\Delta S^0 \quad (18)$$

where K is the sorption equilibrium constant. Values of lnK are obtained by plotting $\ln K_d$ versus C_{eq} and extrapolating C_{eq} to zero

Table 5. Values of thermodynamic parameters for Eu(III) sorption on NRE

T (K)	ΔG^0 (kJ/mol)	ΔS^0 (J/K/ mol)	ΔH^0 (kJ/mol)
303.15	−19.14	177.3	34.61
318.15	−22.34	177.3	34.07
333.15	−24.46	177.3	34.61

(Fig. 9). According to the plots of $\ln K_d$ vs. C_{eq}, K values are 1.986×10^3 mL/g for 30 °C, 4.663×10^3 mL/g for 45 °C, and 6.849×10^3 mL/g for 60 °C, respectively. The thermodynamic parameters mentioned above are tabulated in Table 2.

From Table 2, one can see that the values of standard enthalpy change (ΔH^0) are positive, which indicates that the holistic sorption process is endothermic. Eu(III) is dissolved well in water, and the hydration sheath of Eu(III) is destroyed before its sorption on NRE; this is why this dehydration process needs energy. This energy exceeds the exothermicity of cations to attach to the adsorbent surface. This hypothesis shows that the endothermicity of the desolvation process is higher than the sorption enthalpy by a considerable extent. It is notable that, at 318.15 K (45 °C), the ΔH^0 values of the three processes are all minimum among the three temperatures. This may suggest that the reaction trends to equilibrium gradually with the increase of temperature. Under the conditions applied, sorption is a spontaneous process; as the Gibbs free energy changes (ΔG^0) are negative. With the increase of temperature, the value of ΔG^0 become more negative, and more efficient sorption at high temperature as expected. At high temperature, cations are readily desolvated and hence their sorption is more favorable. The positive values of entropy change (ΔS^0) reflect the affinity of NRE toward Eu(III) ions in aqueous solutions.

7-2. Nonlinear Method

Fig. 10 shows the sorption isotherms by four nonlinear methods mentioned above at different temperatures, and the isotherm parameters are listed in Table 6. From Table 6, it is observed that for two parameters models (Langmuir1 and Freundlich), the Freundlich model could fit the sorption better because of its higher R^2 and lower x^2 at every temperature. To three parameters models (Sips and Toth), Sips

Table 6. Isotherm parameters for Eu(III) sorption on NRE by nonlinear method

t/°C	Langmuir 1				Freundlich			
	c_{max}	b	R^2	x^2	a	n	R^2	x^2
30	0.0023	596.5	0.9172	2.728×10^{-11}	0.5111	0.9074	0.9227	2.550×10^{-11}
45	0.1258	34.21	0.9336	3.7516×10^{-11}	11.18	1.085	0.9375	3.531×10^{-11}
60	1.092×10^{-4}	5.782×10^{4}	0.9229	3.088×10^{-11}	0.0308	0.5809	0.9570	1.723×10^{-11}

t/°C	Sips					Toth				
	c_{max}	b	n	R^2	x^2	c_{max}	b	n	R^2	x^2
30	19.23	0.0184	0.9074	0.9099	2.975×10^{-11}	81.42	0.0162	3	0.9034	3.189×10^{-11}
45	29.71	0.4063	1.085	0.9249	4.238×10^{-11}	146.6	0.0293	3	0.9204	4.498×10^{-11}
60	22.20	1.204	0.581	0.9499	2.009×10^{-11}	119.5	0.024	1.817	0.677	1.294×10^{-10}

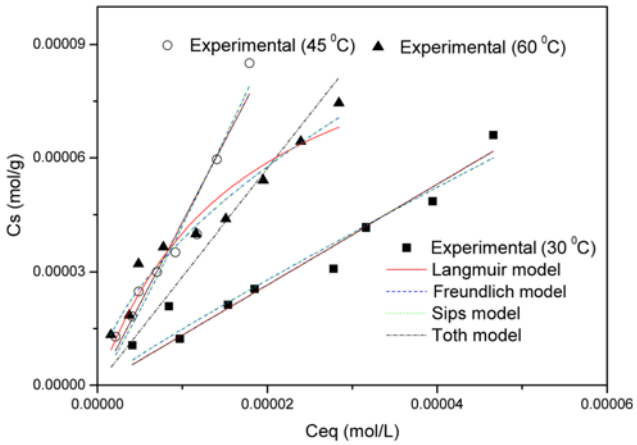

Fig. 10. Nonlinear isotherms of Eu(III) sorption on NRE as a function of temperature. pH=6.50±0.05, m/V=1.0 g/L, I=0.05 mol/L NaCl.

model could fit the sorption better for the same reasons. Compared to three parameters models, two parameters models fit the sorption better.

From Fig. 10, one can see that at different temperature, the fitted curves of Langmuir and Toth models are very close, and the Freundlich and Sips models' fitted curves almost overlap, too. These may be because the Langmuir and Toth models or Freundlich and Sips models have similar expressions. These results indicated that the sorption process could not be described by mono molecule layer sorption model, and the mechanism is complex for the influence of iron oxide and organic matters.

CONCLUSIONS

From the results of Eu(III) sorption on NRE at different experimental conditions, the following conclusions could be drawn:

(1) Sorption of Eu(III) on NRE is strongly dependent on pH and ionic strength. The sorption increases with increasing pH values at pH<7, and then maintains a high level at pH>7.

(2) The time to achieve sorption equilibrium is about 12 hours; the K′ value is 1.169 g/mg/h at 25 °C, and q_e is 5.079 mg/g. The kinetic sorption of Eu(III) on NRE could be described well by a pseudo-second-order model.

(3) Ion exchange or outer-sphere surface complexation may be the main sorption mechanism of Eu(III) on NRE at pH<7, whereas inner-sphere surface complexation may be the main sorption mechanism at pH>7.

(4) The presence of HA enhances the sorption of Eu(III) on NRE at low pH values, and maintains it at high pH values.

(5) Indicated by the thermodynamic parameters, the sorption of Eu(III) on NRE is a spontaneous process; it is an endothermic process in lower temperature range and exothermic process in higher temperature range.

(6) The sorption of Eu(III) on NRE could not be described by simple sorption models. The physicochemical behavior of Eu(III) is dominated by many factors, such as the nature of NRE, humic substances, pH, ionic strength, temperature, *etc*. The sorption isotherms of Eu(III) on NRE could be described by Freundlich model.

(7) The nonlinear method is a better way to describe the sorption isotherm than the linear method, and thus it should be primarily adopted to obtain the adsorption isotherm parameters. Freundlich isotherm model is the best-fit model to the experimental data for the sorption of Eu(III) on NRE.

ACKNOWLEDGEMENTS

Financial support from National Science Foundation of China (No. 20871062 and J1030932), and Fundamental Research Funds for the Central Universities (lzujbky-2010-215) are acknowledged.

REFERENCES

1. D. L. Zhao and C. L. Chen, *J. Radioanal. Nucl. Chem.*, **270**, 445 (2006).
2. L. Chen, X. J. Yu and Z. D. Zhao, *J. Radioanal. Nucl. Chem.*, **274**, 187 (2007).
3. P. Beneš, K. Štamberg, D. Vopálka, L.Široký and Š. Procházková, *J. Radioanal. Nucl. Chem.*, **256**, 465 (2003).
4. K. Štamberg, P. Beneš, J. Mizera, J. Dolanský, D. Vopálka and K. Chalupská, *J. Radioanal. Nucl. Chem.*, **258**, 329 (2003).
5. J. Hu, Zh. Xie, B. He, G. D. Sheng, Ch. L. Chen, J. X. Li, Y. X. Chen and X. K. Wang, *Sci. China Chem.*, **53**, 1420 (2010).
6. X. H. Yu, L. J. Zhu, B. W. Guo and S. Y. He, *Chin. J. Geochem.*, **28**, 220 (2009).
7. W. M. Dong, X. K. Wang, J. Z. Du, X. Y. Bian, F. Ma and Z. Y. Tao,

J. Radioanal. Nucl. Chem., **242**, 793 (1999).
8. Z. Y. Tao, W. J. Li, F. M. Zhang and J. Han, *J. Radioanal. Nucl. Chem.*, **268**, 563 (2006).
9. S. Yu, Z. L. He, C. Y. Huang, G. C. Chen and D. V. Calvert, *J. Environ. Qual.*, **31**, 1129 (2002).
10. K. Mahatantila, Y. Seike and M. Okumura, *Int. J. Eng. Sci. Technol.*, **3**, 1655 (2011).
11. V. Vadivelan and K. Vasanth Kumar, *J. Colloid Interface Sci.*, **286**, 90 (2005).
12. A. E. Ofomaja, *Chem. Eng. J.*, **143**, 85 (2008).
13. S. Chowdhury and P. Saha, *Bioremediat. J.*, **196**, 14 (2010).
14. K. Vasanth Kumar and S. Sivanesan, *J. Hazard. Mater.*, **134**, 277 (2006).
15. K. Štamberg, P. Beneš, J. Mizera, D. Vopálka, Q. H. Fan, D. D. Shao, Y, Lu, W. S. Wu and X. K. Wang, *Chem. Eng. J.*, **150**, 188 (2009).
16. Q. H. Fan, D. D. Shao, Y, Lu, W. S. Wu and X. K. Wang, *Chem. Eng. J.*, **150**, 188 (2009).
17. Q. H. Fan, D. D. Shao, W. S. Wu and X. K. Wang, *Radiochim. Acta*, **96**, 159 (2008).
18. X. K. Wang, Y. X. Chen and Y. C. Wu, *J. Radioanal. Nucl. Chem.*, **261**, 497 (2004).
19. Q. H. Fan, M. L. Zhang, Y. Y. Zhang, K. F. Ding, Z. Q. Yang and W. S. Wu, *Radiochim. Acta*, **98**, 19 (2010).
20. D. D. Shao, Q. H. Fan, J. X. Li, Z. W. Niu, W. S. Wu, Y. X. Chen and X. K. Wang, *Micropor. Mesopor. Mater*, **123**, 1 (2009).
21. M. A. Ferro-Garcýá, J. Rivera-Utrilla, I. Bautista-Toledo and C. Moreno-Castilla, *Langmuir*, **14**, 1880 (1998).
22. S. T. Yang, J. X. Li, Y. Lu, Y. X. Chen and X. K. Wang, *Appl. Radiat. Isot.*, **67**, 1600 (2009).
23. S. Chowdhury R. Misra, P. Kushwaha and P. Das, *Bioremediat. J.*, **15**, 77 (2011).
24. M. Belhachemi and F. Addoun, *Appl. Water Sci.*, **1**, 111 (2011).
25. A. P. Terzyk, J. Chatlas, P. A. Gauden, G. Rychlicki and P. Kowalczyk, *J. Colloid Interface Sci.*, **266**, 473 (2003).
26. L. Chen, B. Gao, S. S. Lu and Y. H. Dong, *J. Radioanal. Nucl. Chem.*, **288**, 851 (2011).
27. R. Donat, G. K. Cılgı, S. Aytas and H. Cetisli, *J. Radioanal. Nucl. Chem.*, **279**, 271 (2009).